JOURNAL OF SOLID STATE CHEMISTRY 110, 305–313 (1994)

Hydrothermal Syntheses, Structures, and Properties of Two New Potassium Vanadium Phosphates: $K_3(VO)(V_2O_3)(PO_4)_2(HPO_4)$ and $K_3(VO)(HV_2O_3)(PO_4)_2(HPO_4)$

J. T. Vaughey, William T. A. Harrison, and Allan J. Jacobson[1]

Department of Chemistry, University of Houston, Houston, Texas 77204-5641

Received April 7, 1993; in revised form August 9, 1993; accepted August 10, 1993

Two new potassium vanadium phosphates have been prepared and their structures have been determined from analysis of single crystal X-ray data. The two compounds, $K_3(VO)(V_2O_3)(PO_4)_2(HPO_4)$ and $K_3(VO)(HV_2O_3)(PO_4)_2(HPO_4)$, are isostructural, except for the incorporation of an extra hydrogen atom into the nearly identical frameworks. The structures consist of a three-dimensional network of $[VO]_n$ chains connected through phosphate groups to a $[V_2O_3]$ moiety. Magnetic susceptibility experiments indicate that in the case of the di-hydrogen compound, there are no significant magnetic interactions between the three independent vanadium (IV) centers. Crystal data: for $K_3(VO)(V_2O_3)(PO_4)_2(HPO_4)$, $M_r = 620.02$, orthorhombic space group *Pnma* (No. 62), $a = 7.023(4)$ Å, $b = 13.309(7)$ Å, $c = 14.294(7)$ Å, $V = 1336(2)$ Å^3, $Z = 4$, $R = 5.02\%$, and $R_w = 5.24\%$ for 1238 observed reflections $[I > 3\sigma(I)]$; for $K_3(VO)(HV_2O_3)(PO_4)_2(HPO_4)$, $M_r = 621.04$, orthorhombic space group *Pnma* (No. 62), $a = 6.975(3)$ Å, $b = 13.559(7)$ Å, $c = 14.130(7)$ Å, $V = 1336(1)$ Å^3, $Z = 4$, $R = 6.02\%$, and $R_w = 6.34\%$ for 1465 observed reflections $[I > 3\sigma(I)]$.

INTRODUCTION

The vanadium phosphate system has been extensively examined since the observation was made that vanadyl pyrophosphate, $(VO)_2P_2O_7$, is an active catalyst for the selective oxidation of butane to maleic anhydride (1–3). Besides studies directed at the elucidation of the catalytic reaction mechanism (4), the synthesis and study of related compounds has aided the understanding of the chemistry of these complex phases (5–12). In particular, a large number of alkali metal vanadium phosphates have been synthesized by a variety of methods, including low and high temperature hydrothermal synthesis (13–18) and high temperature solid state reactions (19). The variety of phases isolated has resulted from the ability of the vanadium cation to exist in several different oxidation states and coordination geometries, as well as the ability of the phosphate anion to have several stable protonated forms. This diversity of environments and coordination polyhedral connectivity has resulted in new phases which exhibit a wide variety of structures and magnetic properties. This paper discusses the structures and properties of two new potassium vanadium phosphates that have been synthesized by low temperature hydrothermal methods, $K_3(VO)(V_2O_3)(PO_4)_2(HPO_4)$ and $K_3(VO)(HV_2O_3)(PO_4)_2(HPO_4)$.

EXPERIMENTAL

Synthesis

$K_3(VO)(HV_2O_3)(PO_4)_2(HPO_4)$. Single crystals of $K_3(VO)(HV_2O_3)(PO_4)_2(HPO_4)$ were isolated as dark green plates in approximately 20% yield from a reaction mixture of initial composition 1.00 g V_2O_5 (98+%, Aldrich), 0.0345 g V (99.9%, Aldrich), 2.0 ml H_3PO_4 (85%, Fisher), and 10 ml distilled H_2O at a pH of 2.80 obtained by dropwise addition of a concentrated solution of KOH. The initial mixture was heated to 220°C for 4 days in a 23-ml Parr bomb and then slowly cooled to room temperature over 2 days. The majority of the reaction mixture was identified as $K_2(VO)_2(HPO_4)_3 \cdot 1.125\ H_2O$ by unit cell determination of a single crystal by X-ray diffraction analysis and by thermogravimetric analysis. The synthesis and structure of this phase was recently reported by Lii and Tsai (18). The compound $K_3(VO)(HV_2O_3)(PO_4)_2(HPO_4)$ was later made in quantitative yield by the stoichiometric reaction of 0.80 g V_2O_5 (98%+, Aldrich), 0.089 g V (99.9%, Aldrich), and 3.0 ml H_3PO_4 (85% solution, Fisher). The pH of the reaction mixture was raised to 4.0 by dropwise addition of a concentrated solution of KOH. The 23-ml Parr bomb was sealed and heated for 4 days at 220°C and then slowly cooled to 25°C over a 2-day period, resulting in a dark green powder identified as $K_3(VO)(HV_2O_3)(PO_4)_2(HPO_4)$ by powder X-ray diffrac-

[1] To whom correspondence should be addressed.

0022-4596/94 $6.00

tion methods. The indexed X-ray powder difraction pattern is listed in Table 1.

$K_3(VO)(V_2O_3)(PO_4)_2(HPO_4)$. Single crystals of $K_3(VO)(V_2O_3)(PO_4)_2(HPO_4)$ were isolated as amber plates from a reaction mixture of initial composition 1.00 g V_2O_5 (98+%, Aldrich), 0.0345 g V (99.9%, Aldrich), 2.0 ml colloidal SiO_2 (Ludox HS-40), 2.0 ml H_3PO_4, and 10 ml distilled H_2O at pH 3.50. This pH was obtained by the dropwise addition of a concentrated solution of KOH to the reaction mixture. The initial mixture was heated to 220°C for 4 days and then slowly cooled to room temperature over a 2-day period. The only phase isolated from the gel, as judged by energy dispersive X-ray analysis (EDX) measurements and visual inspection, was the title compound, $K_3(VO)(V_2O_3)(PO_4)_2(HPO_4)$, as well-faceted single crystals in a wide range of sizes up to 0.4 mm × 0.2 mm × 0.1 mm. Attempts to make this compound in quantitative yield in the absence of the silica gel were unsuccessful.

TABLE 1
Indexed Powder Pattern of $K_3(VO)(HV_2O_3)(PO_4)_2(HPO_4)$[a]

h k l	d_{obs}	d_{calc}	I_{calc}
0 0 2	7.059	7.059	1
0 2 0	6.634	6.678	15
1 0 1	6.229	6.221	44
1 1 1	5.645	5.639	10
1 0 2	4.969	4.945	39
0 2 2	4.853	4.850	6
1 2 1	4.557	4.551	8
0 1 3	4.454	4.438	6
1 3 1	3.625	3.620	31
2 0 1	3.382	3.367	6
1 3 2	3.317	3.309	22
1 0 4	3.162	3.145	30
0 2 4	3.135	3.120	65
2 2 0	3.091	3.075	18
0 4 2/2 1 2/2 2 1	3.020	3.018	100
1 4 1	2.945	2.942	80
1 2 4/2 2 2	2.836	2.845	10
2 0 3	2.801	2.790	25
1 4 2/2 1 3	2.775	2.767	58
0 1 5	2.750	2.762	6
2 3 1	2.697	2.684	6
1 0 5	2.633	2.625	20
2 2 3/1 3 4	2.581	2.574	2
1 1 5/2 2 3	2.565	2.565	15
1 5 1	2.489	2.488	3
2 0 4	2.457	2.454	9
1 2 5/2 1 4	2.434	2.434	1
2 4 0	2.397	2.404	1
2 4 1/2 3 3/0 0 6	2.371	2.370	6
2 4 2	2.265	2.275	9
3 1 1/0 6 0	2.240	2.247	10

[a] Refined orthorhombic cell parameters: a = 6.929(5) Å, b = 13.356(5) Å, c = 14.117(5) Å, V = 1306 Å^3.

Structure Determination

Suitable single crystals of $K_3(VO)(V_2O_3)(PO_4)_2(HPO_4)$ and $K_3(VO)(HV_2O_3)(PO_4)_2(HPO_4)$ were selected for structure determination and mounted on thin glass fibers with epoxy glue. Room temperature (17°C) intensity data were collected using a Nicolet R3m/V automated 4-circle diffractometer (graphite-monochromated Mo$K\alpha$ radiation, λ = 0.71073 Å) for each phase, as outlined in Table 2.

For each phase, 25 reflections were located and centered by searching reciprocal space ($15° < 2\theta < 30°$) and indexed to obtain a unit cell and orientation matrix. The unit cell parameters were optimized by least-squares refinement, resulting in orthorhombic cell constants of a = 7.023(4) Å, b = 13.309(7) Å, c = 14.294(7) Å for $K_3(VO)(V_2O_3)(PO_4)_2(HPO_4)$, and a = 6.975(3) Å, b = 13.559(7) Å, c = 14.130(7) Å for $K_3(VO)(HV_2O_3)(PO_4)_2(HPO_4)$ (digits in parentheses are esds). Intensity data were collected in the $\omega - 2\theta$ scanning mode for $4 < 2\theta < 55°$ with two standard reflections [for $K_3(VO)(V_2O_3)(PO_4)_2(HPO_4)$: (2, −4, 8) and (2, 7, −2); for $K_3(VO)(HV_2O_3)(PO_4)_2(HPO_4)$: (2, 2, 8) and (−4, 3, 3)] monitored every 100 observations for intensity variation; no significant fluctuation in these standards was observed. For both materials, the scan speed was varied from 1.5–14.65°/min, with a scan range of 0.65° below $K\alpha_1$ to 0.65° above $K\alpha_2$.

During data reduction to F and $\sigma(F)$ values, the normal corrections for Lorentz and polarization effects were made. The systematic absences for both materials ($0kl$, $k + l$; $hk0$, h) were compatible with space groups $Pn2_1a$ (No. 33) and *Pnma* (No. 62). For $K_3(VO)(V_2O_3)(PO_4)_2(HPO_4)$, 1789 reflections were measured, of which 1238 were used in the structure solution and refinement [reflections with $I < 3\sigma(I)$ were considered unobserved]. The corresponding values for $K_3(VO)(HV_2O_3)(PO_4)_2(HPO_4)$ were 1797 measured and 1465 observed [$I > 3\sigma(I)$] reflections. An absorption correction based on Ψ-scans (trans min = 0.06, max = 0.10) was applied to the $K_3(VO)(HV_2O_3)(PO_4)_2(HPO_4)$ data.

For both phases, the centrosymmetric space group, *Pnma*, was assumed for the remainder of the crystallographic analysis. One of the vanadium-atom sites in $K_3(VO)(HV_2O_3)(PO_4)_2(HPO_4)$ and one of the phosphorus-atom sites in both $K_3(VO)(HV_2O_3)(PO_4)_2(HPO_4)$ and $K_3(VO)(V_2O_3)(PO_4)_2(HPO_4)$ were found to be disordered over two sites and were modeled as such. In each case, site occupancies were refined, resulting in the parameters reported in Tables 3 and 4. Attempts at refining the structure and modeling the V/P-atom disorder in space group $Pn2_1a$ (No. 33) were undertaken; however, no improvements in the structure resulted. Direct-methods solutions for the heavy-atom (V, P, K) and some of the oxygen-atom positions were obtained from the program

TABLE 2
Crystallographic Parameters

	$K_3(VO)(V_2O_3)(PO_4)_2(HPO_4)$	$K_3(VO)(HV_2O_3)(PO_4)_2(HPO_4)$
Empirical formula	$V_3K_3P_3O_{16}H$	$V_3K_3P_3O_{16}H_2$
Formula wt.	620.02	621.04
Habit	Amber plate	Dark green flat column
Crystal size (mm)	0.40 × 0.20 × 0.07	0.50 × 0.24 × 0.16
Crystal system	Orthorhombic	Orthorhombic
a(Å)	7.023(4)	6.975(3)
b(Å)	13.309(7)	13.559(7)
c(Å)	14.294(7)	14.130(7)
V(Å^3)	1336(2)	1336(1)
Z	4	4
Space group	*Pnma* (No. 62)	*Pnma* (No. 62)
T(°C)	17(2)	17(2)
λ(Mo$K\alpha$) (Å)	0.71073	0.71073
ρ_{calc}(g/cm^3)	3.082	3.086
μ(Mo$K\alpha$) (cm^{-1})	33.72	33.72
Absorption correction	DIFABS	ψ-scans
hkl-data limits	$0 \le 10, 0 \le 18, 0 \le 19$	$0 \le 10, 0 \le 18, 0 \le 19$
Total data ($2\theta < 55°$)	1789	1797
Observed data[a]	1238	1465
Parameters	126	130
$R(F_o)$[b] (%)	5.02	6.02
$R_w(F_o)$[c] (%)	5.24	6.34

[a] $I > 3\sigma(I)$ after merging.
[b] $R = \Sigma||F_o| - |F_c||/\Sigma|F_o|$.
[c] $R_w = [\Sigma w(|F_o| - |F_c|)^2/\Sigma w|F_o|^2]^{1/2}$ with $w_i = 1.0$.

TABLE 3
Atomic Positional Parameters for $K_3(VO)(V_2O_3)(PO_4)_2(HPO_4)$

Atom	x	y	z	U_{eq}[a]
K(1)	0.6263(4)	3/4	0.0083(2)	0.0468
K(2)	0.0976(3)	0.5092(2)	0.6656(1)	0.0461
V(1)	0.1620(2)	0.87564(9)	0.92216(8)	0.0280
V(2)	−0.2488(2)	1/4	0.7594(1)	0.0230
P(1)	0.0347(3)	0.0993(1)	0.8810(1)	0.0242
P(21)[b]	0.365(1)	3/4	0.7605(4)	0.018(2)[c]
P(22)[b]	0.289(1)	3/4	0.7392(4)	0.022(2)[c]
O(1)	0.0245(8)	0.9859(3)	0.8586(3)	0.0307
O(2)	−0.0451(7)	0.8816(3)	1.0121(3)	0.0283
O(3)	0.2806(8)	0.8502(4)	0.7966(3)	0.0367
O(4)	0.3316(7)	0.9371(4)	0.9705(3)	0.0341
O(5)	0.234(1)	3/4	0.9560(4)	0.0277
O(6)	−0.462(1)	1/4	0.8024(4)	0.0245
O(7)	−0.1461(7)	0.1442(4)	0.8395(3)	0.0290
O(8)	0.2157(7)	0.1444(4)	0.8380(3)	0.0282
O(9)	0.423(1)	3/4	0.6553(5)	0.0405
O(10)	0.575(2)	3/4	0.8143(9)	0.0956

[a] U_{eq}(Å^2) = $(U_1U_2U_3)^{1/3}$.
[b] Fractional site occupancies: P(21) = 0.46(1), P(22) = 0.54.
[c] U_{iso}.

TABLE 4
Atomic Positional Parameters for $K_3(VO)(HV_2O_3)(PO_4)_2(HPO_4)$

Atom	x	y	z	U_{eq}[a]
K(1)	0.6324(4)	3/4	0.0014(2)	0.0352
K(2)	0.1103(3)	0.5072(2)	0.6619(1)	0.0325
V(1)	0.1603(2)	0.87885(8)	0.91916(8)	0.0167
V(21)[d]	−0.2419(6)	1/4	0.7596(2)	0.0132(9)[b]
V(22)[d]	−0.1645(9)	1/4	0.7405(3)	0.014(1)[b]
P(1)	0.0451(2)	0.0996(1)	0.8815(1)	0.0146
P(21)[e]	0.378(1)	3/4	0.7591(4)	0.019(2)[b]
P(22)[e]	0.2918(9)	3/4	0.7373(4)	0.017(2)[b]
O(1)	0.0335(7)	0.9905(3)	0.8534(3)	0.0202
O(2)	−0.0522(6)	0.8869(3)	1.0111(3)	0.0184
O(3)	0.2872(7)	0.8448(4)	0.7947(3)	0.0238
O(4)	0.3337(7)	0.9377(4)	0.9677(4)	0.0251
O(5)	0.2310(9)	3/4	0.9688(5)	0.0160
O(6)	−0.4571(9)	1/4	0.8033(5)	0.0170
O(7)	−0.1363(6)	0.1482(3)	0.8423(3)	0.0161
O(8)	0.2265(7)	0.1448(4)	0.8396(4)	0.0220
O(9)	0.428(1)	3/4	0.6548(5)	0.0260
O(10)	0.582(2)	3/4	0.815(1)	0.0968
H(1)	0.23(1)	3/4	1.0395(9)	0.0200[c]

[a] U_{eq}(Å^2) = $(U_1U_2U_3)^{1/3}$.
[b] U_{iso}.
[c] U_{iso} (not refined).
[d] Fractional site occupancies: V(21) = 0.62(1), V(22) = 0.38.
[e] Fractional site occupancies: P(21) = 0.50(1), P(22) = 0.50.

SHELXS-86 (20) and the remaining nonhydrogen atoms were located from Fourier difference maps following refinement of the known atom positions. The least-squares, Fourier, and subsidiary calculations were performed using the Oxford CRYSTALS (21) system, running on a DEC MicroVAX-3100 computer. Final full matrix refinements were against F and included anisotropic temperature factors for the nonhydrogen atoms, and a Larson-type secondary extinction correction (22). An empirical absorption correction (program: DIFABS (23)) was applied to the $K_3V_3HP_3O_{16}$ data after isotropic refinement. Neutral-atom scattering factors, taking into account anomalous dispersion terms, were obtained from the "International Tables" (24).

Final residuals, defined in Table 2, of $R(F) = 5.02\%$ and $R_w(F) = 5.24\%$ ($w_i = 1$) were obtained for $K_3(VO)(V_2O_3)(PO_4)_2(HPO_4)$, and $R(F) = 6.02\%$ and $R_w(F) = 6.34\%$ ($w_i = 1$) for $K_3(VO)(HV_2O_3)(PO_4)_2(HPO_4)$. Difference Fourier maps at the end of the refinement revealed no regions of electron density which could be modeled as an additional atomic site and analysis of the various trends in F_o versus F_c revealed no unusual effects. Tables of anisotropic thermal factors and observed and calculated structure factors are available from the authors as supplementary material.

Final atomic coordinates and thermal parameters are listed in Tables 3 and 4, and selected bond distances and angles are given in Tables 5, 6, 7, and 8.

TABLE 5
Bond Distances (Å) for $K_3(VO)(V_2O_3)(PO_4)_2(HPO_4)$

K(1)–O(2)	2.897(5) × 2	K(1)–O(5)	2.855(7)
K(1)–O(6)	2.941(7)	K(1)–O(8)	2.834(5) × 2
K(1)–O(10)	2.80(1)		
K(2)–O(1)	3.019(6)	K(2)–O(1)	2.806(5)
K(2)–O(3)	2.958(6)	K(2)–O(3)	2.942(6)
K(2)–O(4)	2.991(5)	K(2)–O(4)	2.790(5)
K(2)–O(7)	2.722(5)		
V(1)–O(1)	1.978(5)	V(1)–O(2)	1.943(5)
V(1)–O(3)	2.007(5)	V(1)–O(4)	1.602(5)
V(1)–O(5)	1.812(3)		
V(2)–O(6)	1.619(7)	V(2)–O(6)	2.199(7)
V(2)–O(7)	1.953(5) × 2	V(2)–O(8)	1.994(5) × 2
P(1)–O(1)	1.544(5)	P(1)–O(2)	1.551(5)
P(1)–O(7)	1.524(5)	P(1)–O(8)	1.535(5)
P(21)–O(3)	1.549(6) × 2	P(21)–O(9)	1.557(9)
P(21)–O(10)	1.66(2)		
P(22)–O(3)	1.567(6) × 2	P(22)–O(9)	1.524(9)
P(22)–O(10)	1.69(2)		
P(21)–P(22)	0.616(6)[a]		

[a] Apparent contact due to disorder.

TABLE 6
Bond Distances (Å) for $K_3(VO)(HV_2O_3)(PO_4)_2(HPO_4)$

K(1)–O(2)	2.881(5) × 2	K(1)–O(5)	2.837(7)
K(1)–O(6)	3.019(7)	K(1)–O(8)	2.838(6) × 2
K(1)–O(9)	3.020(8)	K(1)–O(10)	2.65(1)
K(2)–O(1)	2.960(5)	K(2)–O(1)	2.759(5)
K(2)–O(3)	3.079(5)	K(2)–O(3)	3.012(5)
K(2)–O(4)	2.927(5)	K(2)–O(4)	2.763(5)
K(2)–O(7)	2.751(5)		
V(1)–O(1)	1.984(5)	V(1)–O(2)	1.974(4)
V(1)–O(3)	2.022(5)	V(1)–O(4)	1.603(5)
V(1)–O(5)	1.946(3)		
V(21)–O(6)	1.623(7)	V(21)–O(6)	2.176(7)
V(21)–O(7)	1.953(5) × 2	V(21)–O(8)	2.011(5) × 2
V(22)–O(6)	2.226(9)	V(22)–O(6)	1.573(9)
V(22)–O(7)	2.003(5) × 2	V(22)–O(8)	1.973(6) × 2
P(1)–O(1)	1.535(5)	P(1)–O(2)	1.528(5)
P(1)–O(7)	1.530(4)	P(1)–O(8)	1.526(5)
P(21)–O(3)	1.520(6) × 2	P(21)–O(9)	1.514(9)
P(21)–O(10)	1.63(2)		
P(22)–O(3)	1.520(6) × 2	P(22)–O(9)	1.504(8)
P(22)–O(10)	1.64(2)		
O(5)–H(1)	1.00(1)	V(21)–V(22)	0.604(4)[a]
P(21)–P(22)	0.678(6)[a]		

[a] Apparent contact due to disorder.

TABLE 7
Bond Angles (°) for $K_3(VO)(V_2O_3)(PO_4)_2(HPO_4)$

O(2)–V(1)–O(1)	84.7(2)	O(3)–V(1)–O(1)	85.2(2)
O(3)–V(1)–O(2)	155.4(2)	O(4)–V(1)–O(1)	100.5(2)
O(4)–V(1)–O(2)	104.5(2)	O(4)–V(1)–O(3)	99.4(2)
O(5)–V(1)–O(1)	160.6(2)	O(5)–V(1)–O(2)	94.0(2)
O(5)–V(1)–O(3)	88.1(3)	O(5)–V(1)–O(4)	98.6(3)
O(6)–V(2)–O(6)′	178.6(2)	O(7)–V(2)–O(6)	96.8(2)
O(7)–V(2)–O(6)	84.1(2)	O(7)–V(2)–O(7)′	92.3(3)
O(8)–V(2)–O(6)	98.6(2)	O(8)–V(2)–O(6)	80.4(2)
O(8)–V(2)–O(7)	164.5(2)	O(8)–V(2)–O(7)	87.0(2)
O(8)–V(2)–O(8)′	89.6(3)		
O(2)–P(1)–O(1)	111.6(3)	O(7)–P(1)–O(1)	105.3(3)
O(7)–P(1)–O(2)	111.0(3)	O(8)–P(1)–O(1)	109.7(3)
O(8)–P(1)–O(2)	107.0(3)	O(8)–P(1)–O(7)	112.4(3)
O(3)–P(21)–O(3)′	118.9(5)	O(9)–P(21)–O(3)	114.9(3)
O(10)–P(21)–O(3)	100.7(4)	O(10)–P(21)–O(9)	102.6(7)
O(3)–P(22)–O(3)′	116.7(5)	O(9)–P(22)–O(3)	115.8(3)
O(10)–P(22)–O(3)	101.8(4)	O(10)–P(22)–O(9)	101.2(6)
P(1)–O(1)–V(1)	127.3(3)	P(1)–O(2)–V(1)	128.5(3)
P(21)–O(3)–V(1)	127.0(3)	P(22)–O(3)–V(1)	128.8(3)
V(1)–O(5)–V(1)′	134.6(4)	V(2)–O(6)–V(2)′	134.0(3)
P(1)–O(7)–V(2)	145.0(3)	P(1)–O(8)–V(2)	131.3(3)

TABLE 8
Bond Angles (°) for $K_3(VO)(HV_2O_3)(PO_4)_2(HPO_4)$

O(2)–V(1)–O(1)	86.1(2)	O(3)–V(1)–O(1)	87.8(2)
O(3)–V(1)–O(2)	156.0(2)	O(4)–V(1)–O(1)	99.1(2)
O(4)–V(1)–O(2)	104.9(2)	O(4)–V(1)–O(3)	98.9(2)
O(5)–V(1)–O(1)	165.2(2)	O(5)–V(1)–O(2)	90.1(2)
O(5)–V(1)–O(3)	89.9(2)	O(5)–V(1)–O(4)	95.8(3)
O(6)–V(21)–O(6)′	178.3(2)	O(7)–V(21)–O(6)	97.0(2)
O(7)–V(21)–O(6)	84.2(2)	O(8)–V(21)–O(6)	99.4(2)
O(8)–V(21)–O(6)	79.4(2)	O(7)–V(21)–O(7)′	90.0(3)
O(8)–V(21)–O(7)	163.6(3)	O(8)–V(21)–O(7)	87.5(2)
O(8)–V(21)–O(8)′	90.3(3)		
O(6)–V(22)–O(6)′	179.7(3)	O(7)–V(22)–O(6)	78.7(3)
O(7)–V(22)–O(6)	101.1(3)	O(8)–V(22)–O(6)	82.8(3)
O(8)–V(22)–O(6)	97.4(3)	O(7)–V(22)–O(7)′	87.1(3)
O(8)–V(22)–O(7)	161.4(4)	O(8)–V(22)–O(7)	87.2(2)
O(8)–V(22)–O(8)′	92.6(4)		
O(2)–P(1)–O(1)	112.0(3)	O(7)–P(1)–O(1)	106.1(3)
O(7)–P(1)–O(2)	109.6(3)	O(8)–P(1)–O(1)	109.3(3)
O(8)–P(1)–O(2)	108.1(3)	O(8)–P(1)–O(7)	111.8(3)
O(3)–P(21)–O(3)′	115.5(5)	O(9)–P(21)–O(3)	114.7(3)
O(10)–P(21)–O(3)	101.7(4)	O(10)–P(21)–O(9)	106.1(7)
O(3)–P(22)–O(3)′	115.4(5)	O(9)–P(22)–O(3)	115.3(3)
O(10)–P(22)–O(3)	102.9(4)	O(10)–P(22)–O(9)	102.3(7)
P(1)–O(1)–V(1)	126.2(3)	P(1)–O(2)–V(1)	129.4(3)
P(21)–O(3)–V(1)	131.6(3)	P(22)–O(3)–V(1)	131.8(3)
V(1)–O(5)–V(1)′	127.7(3)	V(21)–O(6)–V(21)′	133.6(4)
V(22)–O(6)–V(21)	132.4(3)	V(22)–O(6)–V(22)′	133.4(4)
P(1)–O(7)–V(21)	146.4(3)	P(1)–O(7)–V(22)	129.7(3)
P(1)–O(8)–V(21)	130.3(3)	P(1)–O(8)–V(22)	146.4(4)
P(21)–O(10)–P(21)′	123.7(8)	P(22)–O(10)–P(21)	124.4(7)
P(22)–O(10)–P(22)′	124.4(8)		

Physical Characterization

Thermal analysis was performed on a TA Instruments Hi-Res TGA 2950 thermogravimetric analyzer. The sample was heated to 600°C in flowing oxygen at a rate of 5°C/min. Under these conditions, all of the vanadium atoms in the product are oxidized to the pentavalent state. The total weight change may then be formulated as a combination of the weight gain due to oxygen uptake and the weight loss due to the decomposition of the hydrogen phosphate groups.

Magnetic susceptibility measurements were carried out on an MPMS SQUID susceptometer. The experiments were run using a 1.0-T field in the temperature range 4–300 K. The data were found to obey a Curie–Weiss law and were modeled using the equation $\chi = C/(T - \theta)$.

Powder X-ray diffraction analysis was carried out on a Scintag XDS2000 system. The X-ray powder pattern was indexed using the Scintag "Cell Constants Refinement Program" (25). Calculated intensities, shown in Table 1, were determined by the program LAZY-PULVERIX (26). The starting lattice parameters and positions used in these calculations were the values obtained from the single crystal study.

RESULTS

The structure of the two new potassium vanadium phosphates $K_3(VO)(V_2O_3)(PO_4)_2(HPO_4)$ and $K_3(VO)(HV_2O_3)(PO_4)_2(HPO_4)$ are shown in Figs. 1 and 2. They are composed of two different types of vanadium coordination polyhedra, both commonly seen in vanadium phosphates. One of the two crystallographic vanadium sites, V(2), is in a chain constructed of columns of vanadium/oxygen octahedra running along the *a*-axis of the structure distorted to create a [V=O—V=O] chain. In the dihydrogen compound, $K_3(VO)(HV_2O_3)(PO_4)_2(HPO_4)$, the vanadium octahedra consist of four ≈1.95 Å V–O bonds, one long 2.18 Å V–O bond, and one short ≈1.6 Å vanadyl V=O bond. In this structure, the vanadium octahedra were found to be partially disordered with respect to the direction of the [V=O—V=O] chain, giving the appearance of a column of octahedra with the vanadium cation randomly displaced from the center of the polyhedron. The chain is shown in Fig. 3. In the monohydrogen compound, $K_3(VO)(V_2O_3)(PO_4)_2(HPO_4)$, the chain of octahedra is nearly identical with one short V–O bond of ≈1.6 Å, one long bond of ≈2.20 Å, and four at ≈1.95 Å, but without disorder. The second vanadium coordination environment occurs in a $[V_2O_3]$ unit composed of two corner-sharing vanadium/oxygen square pyramids, as shown in

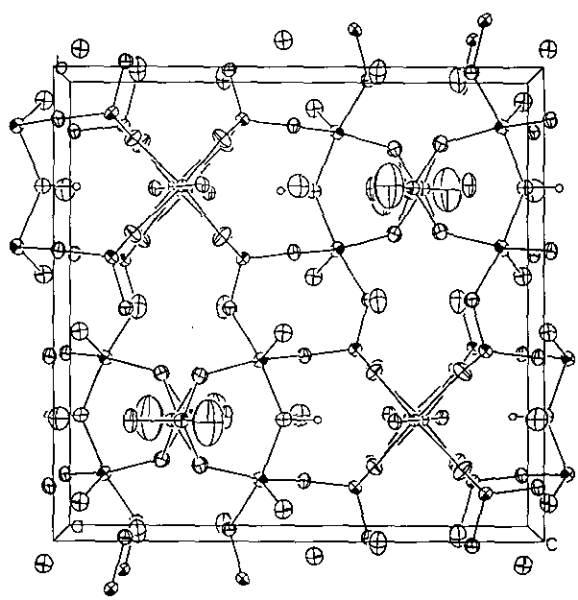

FIG. 1. ORTEP view down the *a*-axis of $K_3(VO)(HV_2O_3)(PO_4)_2(HPO_4)$ with 50% thermal ellipsoids shown. The V and P atoms are shown as shaded ellipses, O and K atoms as open ellipses, and H atoms as plain circles.

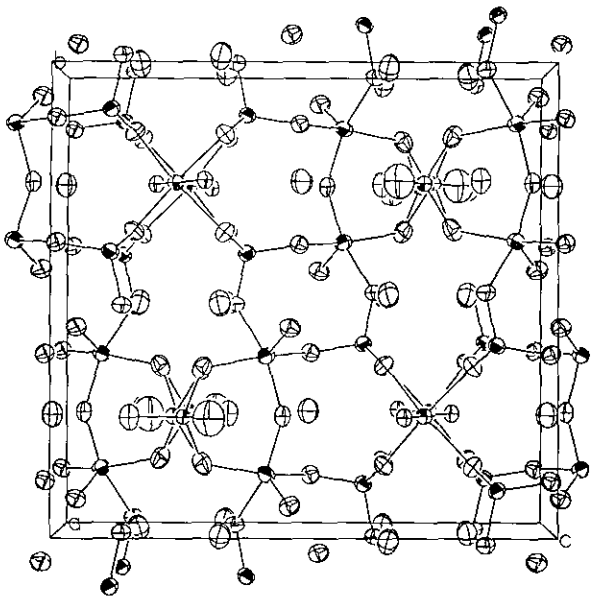

FIG. 2. ORTEP view down the a-axis of $K_3(VO)(V_2O_3)(PO_4)_2(HPO_4)$ with 50% thermal ellipsoids shown. The V and P atoms are shown as shaded ellipses, O and K atoms as open ellipses.

Fig. 4. The difference between the two compounds is within this $[V_2O_3]$ unit; in $K_3(VO)(HV_2O_3)(PO_4)_2(HPO_4)$, the oxygen atom connecting the two square pyramids is protonated, while in $K_3(VO)(V_2O_3)(PO_4)_2(HPO_4)$ it is not. The two different types of vanadium/oxygen coordination polyhedra are connected to each other by phosphate groups such that each phosphate group joins two of the $[V_2O_3]$ dimers to two adjacent vanadium atoms in the nearest $[VO]_n$ chain.

Thermogravimetric analysis of $K_3(VO)(HV_2O_3)(PO_4)_2(HPO_4)$ showed a total weight gain of 0.94%, compared to a calculated weight gain of 0.96% based on the formula $K_3(VO)(HV_2O_3)(PO_4)_2(HPO_4)$. A one-step weight loss occurred at 350°C and was attributed to the

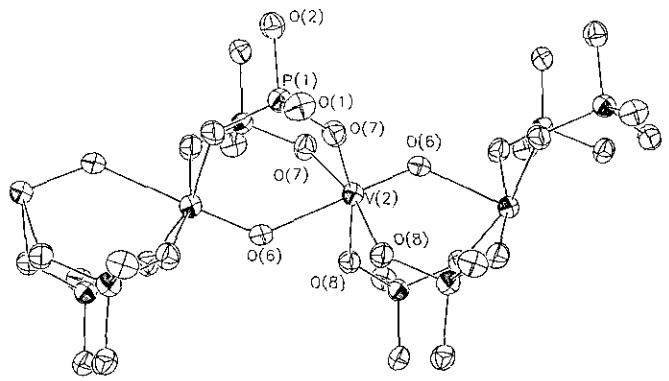

FIG. 3. ORTEP view of the [VO] chain in $K_3(VO)(HV_2O_3)(PO_4)_2(HPO_4)$. The vanadium, phosphorus, and oxygen atoms are shown as 50% thermal ellipsoids.

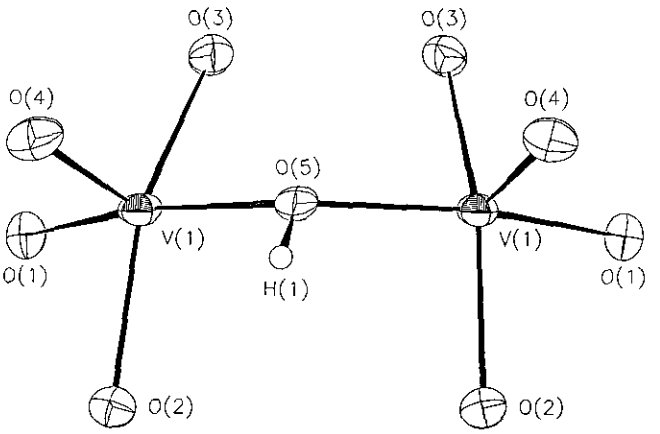

FIG. 4. ORTEP view of the $[HV_2O_3]$ unit in $K_3(VO)(HV_2O_3)(PO_4)_2(HPO_4)$. The vanadium and oxygen atoms are shown as 50% thermal ellipses; the H-atom radius is arbitrary.

decomposition of the hydrogen phosphate group and the loss of the hydrogen on the $[HV_2O_3]$ unit. The weight gain at higher temp (>500°C) was attribued to vanadium cation oxidation. Thermogravimetric analysis of the monohydrogen compound was not possible because of the difficulty of isolating a large enough sample of single crystals completely free from the silica gel.

Magnetic susceptibility measurements were performed on single-crystal samples. The compound $K_3(VO)(HV_2O_3)(PO_4)_2(HPO_4)$ was found to obey a Curie–Weiss-type law and was modeled by the equation $\chi = C/(T - \theta)$. A fit to the magnetic data gave values of $C = 1.28$ emu-K/mol and $\theta = 2.9$ K. The plot is shown in Fig. 5. This Curie value corresponds to 3.2 BM or three unpaired electrons per formula unit, in agreement with the stoichiometry determined from the single crystal experiments. For the compound $K_3(VO)(V_2O_3)(PO_4)_2(HPO_4)$, the very small sample size and difficulty in obtaining a sample free

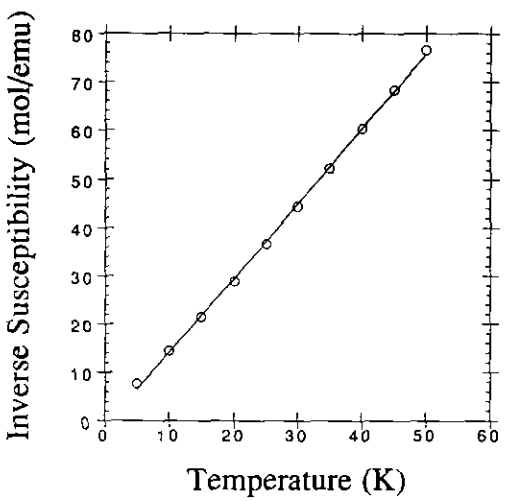

FIG. 5. Plot of inverse magnetic susceptibility versus temperature for $K_3(VO)(HV_2O_3)(PO_4)_2(HPO_4)$.

of SiO_2 (from the preparation) made interpretation of the magnetic data impossible. However, since it has been found to be isostructural with $Tl_3(VO)(V_2O_3)(PO_4)_2(HPO_4)$, a compound of which the magnetic susceptibility data confirm the mixed valent state of the vanadium, no further experiments were undertaken beyond bond valence sum calculations to confirm the oxidation states (13).

Bond valence sum (BVS) calculations were carried out in an effort to assign oxidation states to the vanadium cations and to locate the hydrogen in the hydrogen phosphate group (27), as shown in Table 9. The calculations indicate that the hydrogen atom is most likely attached to O(10), a dangling oxygen atom attached to phosphorus atom P(1). An equivalent position was determined for the thallium analogue (13) by BVS methods. In agreement with the single crystal structure determination, the BVS calculations also suggested that the "extra" hydrogen atom in the dihydrogen compound is located on O(5), the central oxygen atom in the $[V_2O_3]$ unit. The bond valence sum calculations indicate that in the monohydrogen compound, the vanadium atom in the [VO] chain is formally tetravalent, while for the two crystallographically equivalent vanadium atoms in the $[V_2O_3]$ unit, the average is 4.5, or one formally tetravalent and one pentavalent. These assignments agree with the observed stoichiometry and magnetic susceptibility. For the dihydrogen compound, each of the vanadium cations appears to be tetravalent, in agreement with the stoichiometry.

DISCUSSION

Two new K/V/H/P/O materials have been prepared and characterized; $K_3(VO)(V_2O_3)(PO_4)_2(HPO_4)$ is isostructural with the recently reported $Tl_3(VO)(V_2O_3)(PO_4)_2(HPO_4)$ (13), and $K_3(VO)(HV_2O_3)(PO_4)_2(HPO_4)$ differs from it by the addition of a hydrogen atom to the vanadium/oxygen atom framework. The additional hydrogen in the dihydrogen phase was found during the X-ray structural solution and was also identified in bond valence calculations as being on the oxygen atom shared by the vanadium cations in the $[V_2O_3]$ unit. In comparison to the several other potassium vanadium phosphates that have been structurally characterized, these two compounds are constructed of structural moieties common to $K/V/PO_4$ systems. The known compounds and a breakdown of their construction are given in Table 10.

TABLE 9
Bond Valence Sum (BVS) Calculations

	$K_3(VO)(V_2O_3)(PO_4)_2(HPO_4)$		$K_3(VO)(HV_2O_3)(PO_4)_2(HPO_4)$	
	Bond distance	BVS	Bond distance	BVS
O(1)	1.978	0.555	1.984	0.544
O(2)	1.943	0.619	1.974	0.561
O(3)	2.007	0.506	2.022	0.483
O(4)	1.602	1.803	1.603	1.798
O(5)	1.812	0.933	1.946	0.613
Total		4.42		4.00
	V(2) [VO] chain (chain disordered, in the form V21 (V22))			
O(6)	1.619	1.709	1.623 (2.226)	1.688 (0.255)
O(6)	2.199	0.277	2.176 (1.573)	0.298 (1.974)
O(7)	1.953	0.600	1.953 (2.003)	0.600 (0.513)
O(7)	1.953	0.600	1.953 (2.003)	0.600 (0.513)
O(8)	1.994	0.528	2.011 (1.973)	0.500 (0.563)
O(8)	1.994	0.528	2.011 (1.973)	0.500 (0.563)
Total		4.24		4.19 (4.38)
			Weighted Average	4.26
		O(5)		
K(1)	2.885	0.121	2.837	0.125
V(1)	1.812	0.933	1.946	0.613
V(1)	1.812	0.933	1.946	0.613
H(1)	—		1.00	0.736
Total		1.99		2.09
		O(10)		
K(1)	2.800	0.135	2.650	0.184
P(21)	1.660	0.890	1.63	0.973
Total		1.02		1.16

TABLE 10
Known Hydrothermally Synthesized Potassium Vanadium Phosphates

Compound	Temperature of synthesis	Vanadium atom connectivity	Ref.
$K_2(VO)_2(PO_4)(HPO_4)(H_2PO_4)$	450°C	Isolated (VO_6) Octahedra	(18)
$K_{0.5}VOPO_4 \cdot 1.5H_2O$	25°C (powder) 230°C (crystals)	Isolated (VO_6) Octahedra	(31) (16)
$K(VO_2)(HPO_4)$	60°C (powder)	Infinite chains of (VO_5) edge-sharing square pyramids	(14, 15)
$K_2(VO)_3(HPO_4)_4$	240°C	Infinite (VO_6) chains	(17)
$KVOPO_4$	200°C (powder) 700°C (crystals)	Infinite (VO_6) chains	(34)
$K_3(VO)(V_2O_3)(PO_4)_2(HPO_4)$	230°C	Infinite (VO_6) chain and an isolated $[V_2O_3]$ dimer	(This work)
$K_3(VO)(HV_2O_3)(PO_4)_2(HPO_4)$	230°C	Infinite (VO_6) chain and an isolated $[V_2O_3]$ dimer	(This work)

In these two new compounds, the addition of a hydrogen atom to the $[V_2O_3]$ unit, and subsequent formal reduction of a vanadium cation from +5 to +4, was found to have little effect on either the structure or the magnetic properties; that is, no signs of coupling were observed. In the two $[V_2O_3]$ dimers, the V–O–V bond angle decreases from 134.6 to 127.7° upon protonation. The V–O–V bond angle in the thallium analogue, $Tl_3(VO)(V_2O_3)(PO_4)_2(HPO_4)$, is 135.2°. Based on the available literature for vanadyl systems, the unpaired electron lies in the vanadium atom d_{xy} orbital (28), and thus the strongest expected overlap would occur at an angle of ≈135° (29). This is the approximate angle observed for the mixed valent compounds, but larger than that observed for the purely tetravalent compound. A series of well-characterized vanadium (IV) systems in which the structure is built up of $[V_2O_3]$ units is given in Table 11, along with the relevant magnetic and structural data. From a comparison of the limited data in this table, it appears that the more open the V–O–V angle, the stronger the antiferromagnetic interaction. However, such comparisons are difficult because of the limited number of well-characterized compounds and the large difference (≈15°) in the V–O–V angle observed between these compounds and $K_3(VO)(HV_2O_3)(PO_4)_2(HPO_4)$.

TABLE 11
Comparison of $[V_2O_3]$ Units in Known Vanadium (IV) Phosphate Systems

Compound	V–O–V angle	T_N (K)	Ref.
$NaVOPO_4$	142.9(1)	50	(32)
β-$LiVOPO_4$	140.7(2)	40	(33)
$K_3(VO)(HV_2O_3)(PO_4)_2(HPO_4)$	127.7(3)	—	(This work)

Through the use of varied synthetic procedures, two compounds of nearly the same composition and structure were isolated, differing only by one hydrogen atom. Similar results have also been observed in molecular polyoxovanadium chemistry in which, frequently, compounds can be isolated with similar structures but with different average oxidation states due to differing degrees of protonation (30).

ACKNOWLEDGMENTS

We thank the Welch Foundation and the NSF (DMR-9214804) for support, as well as the Texas Center for Superconductivity and Professor Pei Hor for access to the magnetic measurement facilities. We also thank Dr. J. Korp for collecting the X-ray data.

REFERENCES

1. H. Seeboth, H.-J. Freiberg, G. Hopf, J. Kreissig, B. Kubias, G. Ladwig, B. Lucke, G. Muller, and H. Wolf, DDR Patent 113, 210 (1975).
2. H. Seeboth, B. Kubias, H. Wolf, and B. Lucke, *Chem. Tech.* **28,** 730 (1976).
3. E. Bordes and P. Courtine, *J. Chem. Soc. Chem. Commun.* **294** (1985).
4. N. Wustneck, H. Wolf, and H. Seeboth, *React. Kinet. Catal. Lett.* **21,** 497 (1982).
5. G. Ladwig, *Z. Anorg. Allg. Chem.* **338,** 266 (1965).
6. E. Bordes and P. Courtine, *C. R. Seances Acad. Sci., Ser. C* **274,** 1375 (1972).
7. J. W. Johnson, D. C. Johnston, A. J. Jacobson, and J. F. Brody, *J. Am. Chem. Soc.* **106,** 8123 (1984).
8. M. E. Leonowicz, J. W. Johnson, J. F. Brody, H. F. Shannon, Jr., and J. M. Newsam, *J. Solid State Chem.* **56,** 3178 (1985).
9. G. Villeneuve, A. Erragh, D. Beltran, M. Drillon, and P. Hagenmuller, *Mater. Res. Bull.* **21,** 621 (1986).

10. A. LeBail, G. Ferey, P. Amoros, and D. Beltran-Porter, *Eur. J. Solid State Inorg. Chem.* **26,** 419 (1989).
11. A. LeBail, G. Ferey, P. Amoros, D. Beltran-Porter, and G. Villeneuve, *J. Solid State Chem.* **79,** 169 (1989).
12. R. G. Teller, P. Blum, E. Kostiner, and J. A. Hriljac, *J. Solid State Chem.* **97,** 10 (1992).
13. G. Huan, J. W. Johnson, A. J. Jacobson, E. W. Corcoran, Jr., and D. P. Goshorn, *J. Solid State Chem.* **93,** 514 (1991).
14. S. Pulvin, E. Bordes, M. Ronis, and P. Courtine, *J. Chem. Res., Synop.* **29** (1981).
15. P. Amoros, D. Beltran-Porter, A. LeBail, G. Ferey, and G. Villeneueve, *Eur. J. Solid State Inorg. Chem.* **25,** 599 (1988).
16. S. L. Wang, H. Y. Kang, C. Y. Cheng, and K. H. Lii, *Inorg. Chem.* **30,** 3496 (1991).
17. K. H. Lii and H. J. Tsai, *J. Solid State Chem.* **91,** 331 (1991).
18. K. H. Lii and H. J. Tsai, *Inorg. Chem.* **30,** 446 (1991).
19. V. C. Korthuis, R. D. Hoffmann, J. Huang, and A. W. Sleight, *Chem. Mater.* **5,** 206 (1993).
20. G. M. Sheldrick, SHELXS-86 User Guide, Crystallography Department, Univ. of Gottingen, Germany, 1986.
21. J. R. Carruthers, D. J. Watkins, and P. W. Betteridge, CRYSTALS User Guide, Chemical Crystallography Laboratory, Oxford Univ. 1990.
22. A. C. Larson, *in* "Crystallographic Computing" (F. R. Ahmed, Ed.), p. 291. Munksgaard, Copenhagen, 1970.
23. N. Walker and D. Stuart, *Acta Crystallogr. Sect. A* **39,** 158 (1983).
24. D. T. Cromer, "International Tables for X-Ray Crystallography," Vol. IV, Table 2.3.1. Kynock, Birmingham, 1974.
25. "Cell Constants Refinement Program," Version 2.20-MVMS. Scintag/USA, Sunnyvale, CA, 1992.
26. Y. Yvon, W. Jeitschko, and E. Parthe, *J. Appl. Crystallogr.* **10,** 73 (1977).
27. I. D. Brown, *in* "Structure and Bonding in Crystals" (M. O'Keefe and A. Navrotsky, Eds.), Vol. II. Academic Press, New York, 1981.
28. A. Syamal, *Coord. Chem. Rev.* **16,** 309 (1975).
29. J. B. Goodenough, *in* "Magnetism and the Chemical Bond." Wiley, New York, 1963.
30. G. Huan, A. J. Jacobson, and V. W. Day, *Angew. Chem.* **103,** 56 (1991); *Angew. Chem. Int. Ed. Engl.* **30,** 422 (1991).
31. J. W. Johnson and A. J. Jacobson *Angew. Chem.* **95,** 422 (1983); *Angew. Chem. Int. Ed. Engl.* **22,** 412 (1983).
32. K. H. Lii, C. H. Li, T. M. Chen, and S. L. Wang, *Z. Kristallogr.* **197,** 67 (1991).
33. K. H. Lii, C. H. Li, C. Y. Cheng, and S. L. Wang, *J. Solid State Chem.* **95,** 352 (1991).
34. M. L. F. Phillips, W. T. A. Harrison, T. E. Gier, G. D. Stucky, G. V. Kulkarni, and J. K. Burdett, *Inorg. Chem.* **29,** 2158 (1990).